



Scholars Research Library

Der Pharma Chemica, 2015, 7(2):12-24  
(<http://derpharmachemica.com/archive.html>)



ISSN 0975-413X  
CODEN (USA): PCHHAX

## Investigation of isomers of hydroxyphenylamino propane nitrile as mild steel corrosion inhibitors in 1M HCl

M. El Azzouzi<sup>1\*</sup>, A. Aouniti<sup>1</sup>, L. Herrag<sup>1</sup>, A. Chetouani<sup>1,2</sup>, H. Elmsellem<sup>1</sup> and B. Hammouti<sup>1,3</sup>

<sup>1</sup>Laboratoire de Chimie Appliquée et environnement (LCAE-URAC18), Faculté des Sciences, Oujda, Morocco

<sup>2</sup>Laboratoire de chimie physique, Centre Régionale des Métiers de l'Education et de Formation "CRMEF", Région de l'Orientale, Oujda, Morocco

<sup>3</sup>Chemistry Department, Faculty of Science, Taibah University, Saudi Arabia

### ABSTRACT

The inhibition effect of 3-(4-Hydroxyphenylamino) propanenitrile (Para) and 3-(2-Hydroxyphenylamino) propanenitrile (ortho) on the corrosion of steel mild 1M HCl solution was studied by weight loss, potentiodynamic polarization and electrochemical impedance spectroscopy methods. The results revealed that corrosion rate depends on the molecular structure and the concentration of inhibitors. We found that the Para Hydroxyphenylamino propanenitrile is a good inhibitor and has been tested with efficiency reaches to 85% in  $10^{-3}$ M. Polarization studies through electrochemical curves and spectroscopy of electrochemical impedance clearly show that 3-(4-Hydroxyphenylamino) propanenitrile is a mixed inhibitor. The adsorption of Ortho and Para inhibitors on the mild steel surface obeys Langmuir isotherm. Both thermodynamic parameters (adsorption heat  $\Delta H^\circ$ , adsorption free energy  $\Delta G^\circ$  and adsorption entropy  $\Delta S^\circ$ ) and kinetic parameters (apparent activation energy  $E_a$ ) were calculated and discussed. The quantum chemical parameters calculated using DFT at the B3LYP/6-31G\* level of theory show a good correlation to the inhibition efficiency. The highest occupied molecular orbital (HOMO), the lowest unoccupied molecular orbital (LUMO), the separation energy ( $\Delta E$ ) and the dipole moment ( $\mu$ ) from the inhibitor to the metal surface explain well experimental data.

**Keywords:** Corrosion, acid, inhibitor, nitrile, amine, steel, Weight loss, EIS, DFT.

### INTRODUCTION

The use of water as thermal fluid in cooling water system usually leads to three problems namely: scale, corrosion and biological fouling processes. These phenomena are the cause of lower thermal efficiency of the circuit, loss of the metallic material and the growth of microorganisms in water. The economic losses caused by these problems are for the most part huge and consistent. To limit the damage, many formulations have been developed to protect circuits, piping and materials structures against this scourge. Many researches has been performed to study corrosion inhibitions of many inhibitors on mild steel in HCl media using organic compounds [1,2], that necessary is due to the massive annuels degradation of steel by corrosion. Inhibitors are often used in thos process to control the metal dissolution [3-5]. Hydrochloric acid is widely used in the pickling, cleaning and descaling of steel and ferrous alloys[6-8]. A lot of studies has proved that we can reach till the great efficiencies by using some organic inhibitors, it depend on their moleculaire structureur (containingnitrogen, sulfur, and oxygen atoms; the presence of  $\pi$ -electrons) which induce a greateradsorption of the inhibitor molecules onto the surface of the metal.[9-18]. This can be explained by the formation of a relatively compact film on metallic surface. It was also shown that the inhibition properties of this film remain independent of hydrodynamic conditions and is reinforced with the immersion time. The inihibition of corrosion is related to block one of oxydation reaction or reduction reaction or both of them by the adsorption mechnisme. More work in our laboratory, realized a correlation between experimental efficiencies of inhibitors and the results of quantum chemical calculations, and constructed a composite index of some of the key

quantum chemical parameters in order to characterize the inhibition performance of the tested molecules. The quantum calculations tend to correlate the effect of structural parameters of two mesomer of Hydroxyphenylamino propanenitrile ortho and para to their inhibition efficiencies of corrosion of steel in HCl solution. Molecular orbital calculations are performed looking for good theoretical parameters to characterize the inhibition property of inhibitors, which will be helpful to gain insight into the mechanism of corrosion inhibition and then to simulate the adsorption mode of the inhibitor on the metal surface. During this study we have tested two mesomer of Hydroxyphenylamino propanenitrile HPAPN as inhibitors of steel's corrosion, we used a different methods such as weight loss and electrochemical study, beside detailed investigation of temperature and immersion time effects was also studied and discussed to more understanding the adsorption mechanism of the studied inhibitors.

## MATERIALS AND METHODS

### 1.1. Materials

The material used in this study was mild steel, C38 carbon, with a chemical composition (in wt %) of 0.09 % P; 0.38 % Si; 0.01 % Al; 0.05 % Mn; 0.21 % C; 0.05 % S and the remainder iron (Fe). Two batches of tests were performed, we report here on the average values.

### 1.2. Inhibitors

Both position isomers of Hydroxyphenylamino propanenitrile were synthesised in our laboratory. The tested compounds were characterized by IR,  $^1\text{H-NMR}$  and  $^{13}\text{C-NMR}$  and mass spectrometry before using and characterised, Fig 1 shows their structure moleculaire

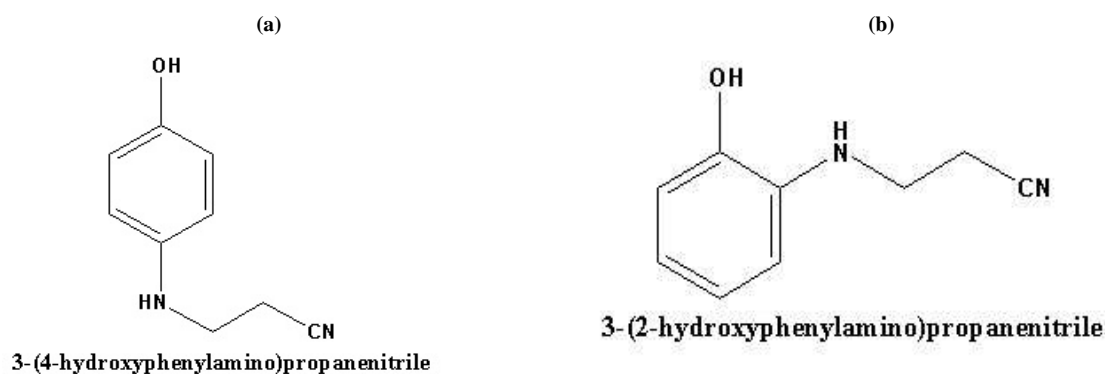


Fig. 1 : Chemical molecular structure of Para (a) and ortho (b) position

### 1.3. Solutions

The aggressive solutions, 1.0 M HCl were prepared by dilution of AR grade 37% HCl with distilled water. The concentration range of inhibitors employed was  $10^{-3}$ - $10^{-6}$  mol.l $^{-1}$ .

### 1.4. Weight loss

The experiments were carried out in the solution of HCl 1M on mild steel, the sheets with the dimensions of 1.5cm x 1.5cm x 0.25cm were abraded with a series of emery paper (grade 180-400-800-1200), washed with distilled water and dried. After weighing accurately, the sheets were immersed in a glasse beackers contained 50ml of Hydrochloric acid 1M with and without presence of different concentration of inhibitors under 308°K temperatur, after 6 hours, the specimens were taken out from the vessel, wached by distilled water, dried and weighted accuratly [9], in order to get a good reproducibility, expirements were carried out in triplicate. The following equation represent the formula to calculate corrosion rate ( $w$ ) :

$$w = \frac{\Delta m}{S \times t} \quad (1)$$

$\Delta m$  represent the weight loss (difference in mass before and after immersed),  $S$  the total area for each sheet, and  $t$  is immersion time (6 h). With the calculated corrosion rate, the inhibition efficiency ( $IE_w$ ) was calculated through the following equation, where  $v_0$  and  $v$  are the values of the corrosion rate without and with presence of the inhibitors, respectively.

$$\%IE_w = \frac{v_0 - v}{v_0} \times 100 \quad (2)$$

### 1.5. Electrochemical measurements:

The electrochemical study was carried out by using the polarization potentiodynamic method on PGZ100 controlled by a pc supported Master Lab 4software. The experiments were performed in a conventional three-electrode cylindrical Pyrex glass cell. The temperature is thermostatically controlled at 308 K. The working electrode (WE) in the form of disc cut from steel has a geometric area of 1 cm<sup>2</sup> and is embedded in polytetrafluoro ethylene (PTFE). A saturated calomel electrode (SCE) and a platinum electrode were used, as reference and auxiliary electrodes, respectively. A fine Lugging capillary was placed close to the working electrode to minimize ohmic resistance [5,17]. During each experiment, the test solution was mixed with a magnetic stirrer and the gas bubbling was maintained. The mild steel electrode was maintained at corrosion potential for 30 min and thereafter pre-polarized at -800 mV for 10 min. The potential was swept to anodic potentials by a constant sweep rate of 0.5 mV s<sup>-1</sup>.

The working surface area was abraded with emery paper (grade 600-800-1200) on the test face, rinsed with distilled water, and dried. Before measurement the electrode was immersed in test solution at open circuit potential (OCP) for 30 min until a steady state was reached. Each experiment was repeated at least three times to check the reproducibility.

The potential of potentiodynamic polarization curves was increased for 10min and started from a potential of -800 mV to -200mV vs. free corrosion potential ( $E_{corr}$  vs. SCE).  $IE_p\%$  was defined as:

$$IE_p\% = \frac{I_{corr} - I_{corr(inh)}}{I_{corr}} \times 100 \quad (3)$$

Where  $I_{corr}$  and  $I_{corr(inh)}$  represent the corrosion current density values without and with inhibitor, respectively.

The electrochemical impedance spectroscopy (EIS) measurements were carried out with the electrochemical system (Tacussel) which included a digital potentiostat model Volta lab PGZ 100 computer at Ecor after immersion in solution without bubbling. Electrochemical impedance spectroscopy (EIS) was carried out after 30 min of immersion, in the frequency range of 0.1 Hz - 100 kHz using a 10 mV peak-to-peak voltage excitation. The impedance diagrams are given in the Nyquist representation. Before recording the curves, the test solutions were de-aerated in magnetically stirred for 30 min in the cell with nitrogen.  $IE_{Rt}\%$  was defined as:

$$IE_{Rt}\% = \frac{R_t(inh) - R_t(0)}{R_t(inh)} \times 100 \quad (4)$$

Where  $R_t(0)$  and  $R_t(inh)$  are charge transfer resistance for CRS in the absence and presence of inhibitor, respectively [4,19].

### 1.6. Quantum chemical calculation :

In order to correlate theoretical study with experimental results found by gravimetric and electrochemical methods, the geometrical optimization of inhibitors were performed by DFT (density functional theory) using the hybrid functional B3LYP level taking into account the exchange and the correlation with Beck's three parameters exchange functional along with Lee et al. non-local correlation functional with 6.31G (d,p) basis set is implemented in Gaussian03 program package, the following quantum chemical parameters such as  $E_{HOMO}$ ,  $E_{LUMO}$ ,  $\Delta E = E_{LUMO} - E_{HOMO}$  and Dipole moment  $\mu$  were obtained from the optimized structure that can be related to the metal-inhibitor interactions [20-22].

## RESULTS AND DISCUSSION

### 1.7. Weight loss measurements

#### 1.7.1. Effect of inhibitors on the corrosion rate

The corrosion rate values of mild steel by addition of inhibitors in 1M hydrochloric acid are listed in Table 1.

It shows clearly that the corrosion rate decrease by increasing the concentration for both molecules, the inhibition efficiency increase by increasing the concentration and reach until 85% in para position at a concentration of 10<sup>-3</sup>M, as we know, the benzene ring is an excellent carrier of electrons, the greater the number of electrons around the nitrogen the stronger bond which is formed between the nitrogen and the metal, the function of the hydroxyde group is an electron attracture which include an interaction between amine and hydroxyde functions in ortho position, and thus increase the electron density in the nitrogen atom of the vinyl.[16].

**Table 1: Corrosion rate and efficiencies values of different concentrations of both position isomers of Hydroxyphenylamino propanenitrile in HCl 1M media**

Inhibitors	Concentration (mol.l <sup>-1</sup> )	Corrosion rate (mg.cm <sup>-2</sup> .h <sup>-1</sup> )	Efficiency (%)
Blank	1M	6.2	—
Ortho	10 <sup>-6</sup>	5.86	5.37
	10 <sup>-5</sup>	5.08	17.96
	5.10 <sup>-5</sup>	4.15	32.98
	10 <sup>-4</sup>	4.03	34.97
	5.10 <sup>-4</sup>	2.62	57.61
	10 <sup>-3</sup>	2.20	64.38
Para	10 <sup>-6</sup>	4.63	25.25
	10 <sup>-5</sup>	3.58	42.25
	5.10 <sup>-5</sup>	1.58	74.50
	10 <sup>-4</sup>	1.07	82.68
	5.10 <sup>-4</sup>	0.92	85.02
	10 <sup>-3</sup>	0.90	85.38

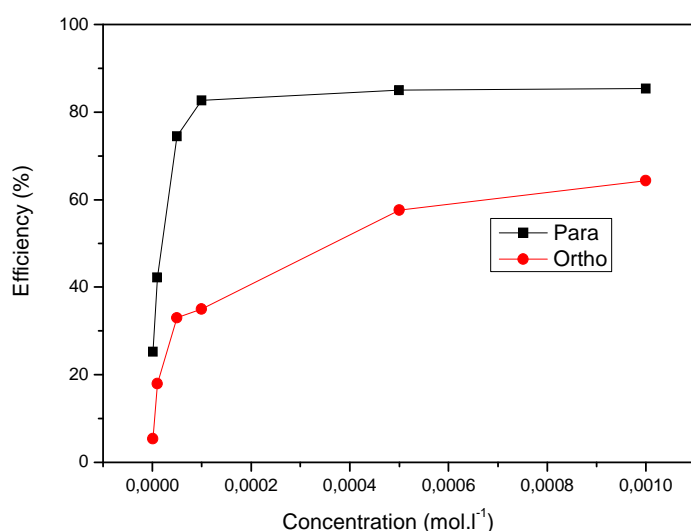
**Fig. 2 Variation of the inhibition efficiency with Para and Ortho inhibitor concentrations for the steel in 1M HCl**

Fig. 2 illustrates the variation of the inhibition efficiency ( $E_w\%$ ) versus the concentration for both molecules. Inspection of these data reveals that the protection efficiency increases with increasing the concentration of the inhibitor and reaches a maximum (85 %) and (64%) at  $10^{-3}$  M for para and ortho position respectively. The corrosion inhibition can be attributed to the adsorption of para molecule at the steel acid solution interface. We can conclude that the efficiency of inhibitors follow the order : Para > Ortho

### 1.7.2.Effect of inhibitors concentration and temperature on inhibition efficiency

The relationship between temperature and the inhibition efficiency of Ortho and para of HAPPN compounds on the corrosion of steel in 1M HCl solution tested at different temperature (30°C, 40°C, 50°C and 60°C) in weight loss tests. Table 2, regroups the results of weight loss of steel in 1M HCl with and without the addition for the concentration that gave us the great efficiency for both molecules, it is very clear that as we increase the temperature the corrosion rate decrease, it also shows that HAPPN in para position can resist a little bit in high temperature, in the opposite the HAPPN in ortho position seems like useless. The Fig. 3 shows the evolution of the inhibition efficiency of the HAPPN compounds by increase temperature for both molecules By using Arrhenius equation and its alternative formulation called transition state equation (5), it is possible to calculate activation thermodynamic parameters of the corrosion process such as activation energy  $E_a$ , activated entropy  $\Delta S_a$  and enthalpy  $\Delta H_a$ :

$$\ln(v) = \ln(A) - \frac{E_a}{RT} \quad (5)$$

$$\ln\left(\frac{v}{T}\right) = \left(\ln\left(\frac{R}{Nh}\right) + \frac{\Delta S_a}{R}\right) - \frac{\Delta H_a}{RT} \quad (6)$$

Where  $v$  is the corrosion rate,  $A$  is a constant depends on metal type and electrolyte,  $E_a$  is the apparent activation energy,  $h$  is the Planck's constant ( $6.626176 \times 10^{-34}$  Js),  $N$  is the Avogadro number ( $6.02252 \times 10^{23}$  mol<sup>-1</sup>),  $R$  is the universal gas constant and  $T$  is the absolute temperature,  $\Delta H_a$  and  $\Delta S_a$  are the the enthalpy and the entropy of activation, respectively.

**Table 2: Corrosion rate value of the corrosion of mild steel in HCl 1M media with and without inhibitors in different temperature**

Compounds	Temperature (°K)	Concentration (mol.l <sup>-1</sup> )	Corrosion Rate (mg.cm <sup>-2</sup> .h <sup>-1</sup> )	Efficiency (%)
HCl	313	1	14.76	-
	323	1	16.42	-
	333	1	18.08	-
	343	1	23.41	-
Ortho	313	10 <sup>-3</sup>	5.87	60.19
	323	10 <sup>-3</sup>	11.14	32.12
	333	10 <sup>-3</sup>	13.20	26.94
	343	10 <sup>-3</sup>	25.72	09.20
Para	313	10 <sup>-3</sup>	2.73	81.46
	323	10 <sup>-3</sup>	4.42	73.07
	333	10 <sup>-3</sup>	8.04	55.52
	343	10 <sup>-3</sup>	13.68	41.52

Obviously, from the equation (5), the activation energy is the slope  $-E_a/R$  by plotting the logarithme of corrosion rate versus  $1/T$ . Fig. 4 shows the variation of logarithme of the corrosion rate with and without presence of inhibitors with the reciprocal of absolute temperature

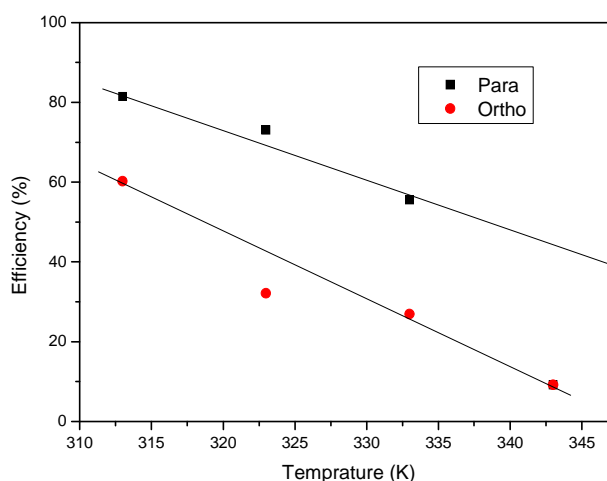


**Fig.3 the plots of E% vs Temperature of Ortho and Para inhibitors on the surface of steel in 1M HCl**

The activation energy of steel in 1M HCl in the presence and absence of the two position isomers is listed in Table 3, we observe that  $E_a$  is higher in inhibited slution, it reach until 45,643 kJ mol<sup>-1</sup> in para position[12],

**Table 3: The values of activation parameters for steel in 1M HCl with and without presence of HAPPN position isomers**

Compounds	Concentration	$E_a$ (kJ mol <sup>-1</sup> )	$\Delta H_a$ (kJ mol <sup>-1</sup> )	$\Delta S_a$ (kJ mol <sup>-1</sup> )	$E_a - \Delta H_a$
HCl	1	1	13,107	10,385	190,016
Ortho	10 <sup>-3</sup>	10 <sup>-3</sup>	41,009	38,286	108,031
Para	10 <sup>-3</sup>	10 <sup>-3</sup>	48,365	45,643	91,428

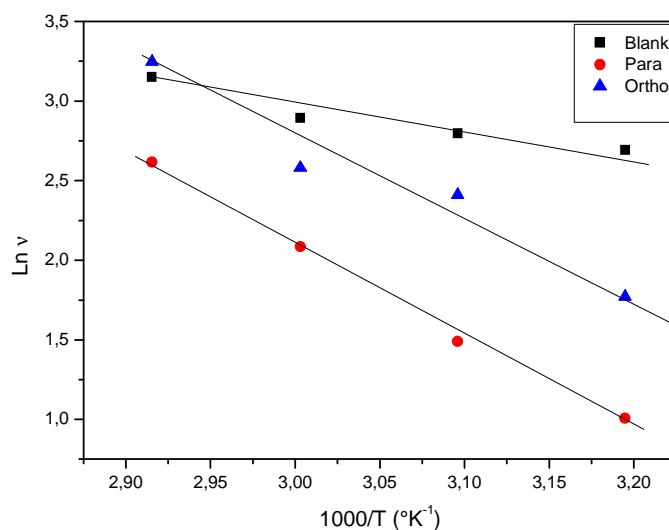


Fig. 4 Arrhenius plots of Ortho and Para inhibitors on the surface of steel in 1M HCl

For the thermodynamic parameters ( $\Delta H_a$  and  $\Delta S_a$ ), the plots of  $\ln(v/T)$  vs  $1/T$  give a straight line with a slope of  $\Delta H_a/R$  and an intercept of  $(\ln(R/Nh) + (\Delta S/R))$  as shown in Fig. 5

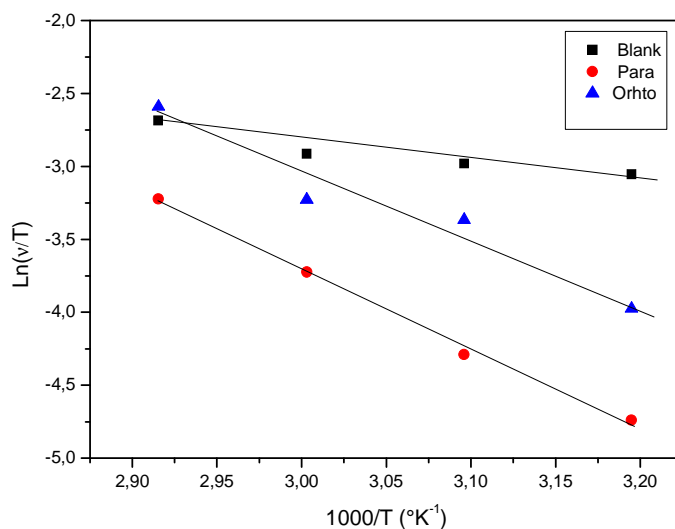


Fig. 5: the plots of  $\ln(v/T)$  vs  $1/T$  of Ortho and Para inhibitors on the surface of steel in 1M HCl

By employing equation (6), the activation enthalpy  $\Delta H_a$  and entropy  $\Delta S_a$  are calculated and illustrated also in Table 3. The positive values of  $\Delta H_a$  mean that the dissolution reaction is an endothermic process, the entropy of activation  $\Delta S_a$  decrease from the uninhibited solution to the inhibited solution [13].

As the activation energy and enthalpy increase the inhibition efficiency, that could be explained by an increase of the energy barrier of corrosion. In case of endothermic adsorption enthalpy, with a high activation energy barrier for the transition between strongly bonded  $H_{ads}$  and  $H_{diss}$  [11].

We can see from Table 3 that the difference between  $E_a$  and  $\Delta H_a$ s and respect the following equation :

$$E_a - \Delta H_a = RT \quad (7)$$

The results shows that the inhibitor acted equally on the activation energy and activation enthalpy.

**1.7.3. Adsorption isotherm of HAPPN on the mild steel surface**

Many informations could be read out from the adsorption isotherm, because it mainly depends on the interaction between inhibitor and surface of metal.

There are many adsorption isotherms such as:

$$\text{Langmuir isotherm} \quad \frac{\theta}{(1-\theta)} = K_{ads} \times C \quad (8)$$

$$\text{Temkin isotherm} \quad e^{f\theta} = K_{ads} \times C \quad (9)$$

$$\text{Frumkin isotherm} \quad \frac{\theta}{(1-\theta)} \times e^{-2f\theta} = K_{ads} \times C \quad (10)$$

$$\text{and Freundlich isotherm} \quad \theta = K_{ads} \times C \quad (11)$$

Where  $k_{ads}$  is the equilibrium constant of the adsorption process,  $C$  the inhibitor concentration and  $f$  the factor of energetic inhomogeneity. The simplest one is that of Langmuir which involves assumptions of (a) no interactions between the adsorbed species on the electrode surface, (b) no heterogeneity of the surface, and (c) at high bulk activities, saturation coverage of the electrode by adsorbate (e.g., to form a monolayer) of surface coverage  $\theta$ .

The plot of  $C_{inh}/\theta$  versus  $C_{inh}$  is a straight line with nearly unit slope and the best fits are obtained with Langmuir adsorption isotherm as presented in Fig. 6, the linear correlation coefficient is almost 1.00 which proves that both molecules obey the Langmuir adsorption isotherm [6].

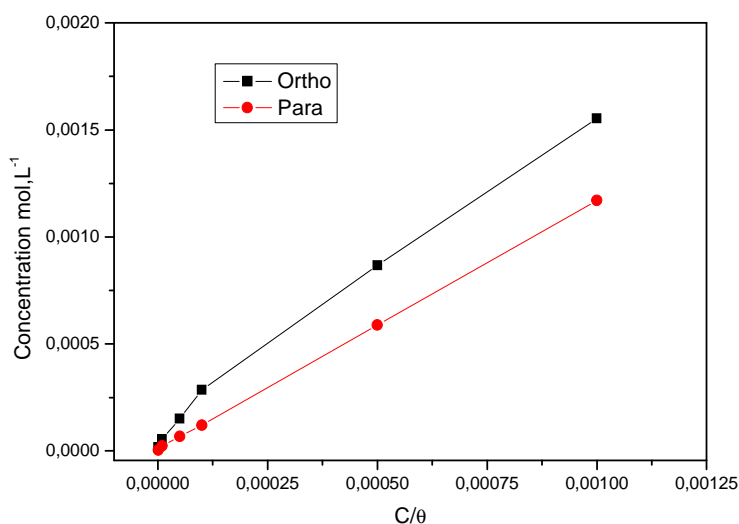


**Fig. 6 Langmuir isotherm adsorption model of Ortho and Para inhibitors on the surface of steel in 1M HCl**

To extract the thermodynamic parameters, we needed to draw the linear regression between  $C$  and  $C/\theta$ , as we mentioned previously, using Microsoft Office Excel Software, the straight line is expressed by the following equation:

$$\frac{C}{\theta} = \frac{1}{K} + C \quad (12)$$

Where  $C$  is the concentration of inhibitor,  $K$  is the adsorptive equilibrium constant.

We obtained  $K$  from the intercepts of the straight line  $C_{inh}/\theta -$  axis, which lead us to calculate the standard free energy of adsorption  $\Delta G_{ads}^\circ$  by the following equation:

$$\Delta G_{ads}^\circ = -RT \cdot \ln(55.5 \cdot K) \quad (13)$$

**Table 4: Parameter thermodynamiques of adsorption of inhibitors on the steel mild in HCl 1M**

Compounds	Linear correlation	Slope	Intercept	K	$\Delta G^\circ(\text{kJ mol}^{-1})$
Ortho	0.9930	1,5099	$7,04.10^{-3}$	$1,42.10^4$	-34,767
Para	0.9999	1,1639	$6,76.10^{-6}$	$1,48.10^5$	-40,769

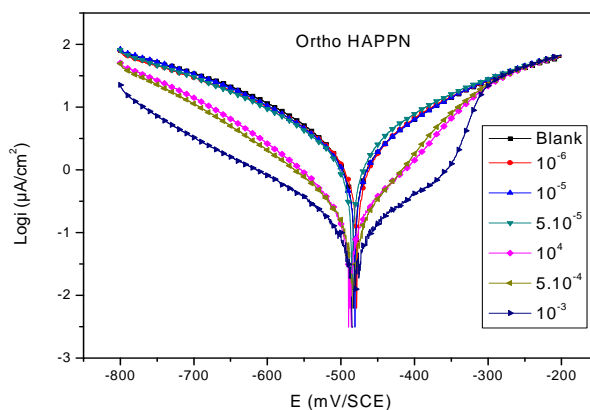
Where  $R$  is the universal gas constant and  $T$  is the absolute temperature, the results of standard free energy of adsorption are listed in Table 4,  $\Delta G^\circ_{\text{ads}}$  are  $-40,679 \text{ kJ mol}^{-1}$  and  $-34,783 \text{ kJ mol}^{-1}$  for HAPPN *Ortho* and *Para* respectively, the negative values of  $\Delta G^\circ_{\text{ads}}$  prove that adsorption process goes spontaneous and the adsorbed layer on the steel surface. In the Table 4, it is well known that values of  $\Delta G^\circ_{\text{ads}}$  of the order of  $20 \text{ kJ mol}^{-1}$  or lower indicate a physisorption; those of order of  $40 \text{ kJ mol}^{-1}$  or higher involve charge sharing or transfer from the inhibitor molecules to the metal to form a coordinate type of bond chemisorption. [10]

Hence it can be suggested that each inhibitor adsorbs on the metallic surface forming strong chemisorption bonds. This is in fact possible in view of the presence of unshared electron pairs in the organic compounds molecules and taking into consideration the behaviour of iron as an electron acceptor as its d-sub monolayer is incomplete. The inhibitors studied may then be adsorbed via donor-acceptor interactions between the  $\pi$ -electrons of the aromatic systems and the unshared electron pairs of the heteroatom's (-N, -O) to form a bond with the vacant d orbital of the C38 steel atom on the metal surface, which acts as a Lewis acid, leading to the formation of a protective chemisorbed layer. The presence of a cyclic group (which releases electrons) in the inhibitor molecule will increase the electron density on the active centre of the molecule and good protection will occur. In the case of inhibitor *Para* (with a withdrawing group) the reverse will occur, this will explain the previous results.

We concluded effectively that the fact that the inhibition phenomenon for the *Para* HAPPN position isomers example, can be imputed to the presence of empty d-orbitals in the Fe which led to an easier coordinate bond formation between the metal and inhibitors. Therefore, physical adsorption is also possible via electrostatic interaction between a negatively charged surface, which is provided with a specifically adsorbed chloride anion on C38 steel, and the positive charge of the inhibitors.

#### 1.7.4. Polarization measurements

An electrochemical study was carried out to study the polarization behaviour of steel in 1 M HCl in the presence and the absence of HAPPN position isomers in Fig. 7 and Fig. 8. The electrochemical parameters such as the corrosion current density ( $I_{\text{corr}}$ ), corrosion potential ( $E_{\text{corr}}$ ), cathodic Tafel slope ( $\beta_c$ ), anodic Tafel slope ( $\beta_a$ ) and inhibition efficiency ( $E_i\%$ ) obtained from polarization measurements are calculated and illustrated in Table 5.

**Fig. 7: Polarization curves of steel mild in 1.0 M HCl with and without different concentrations of Ortho at 308 K**

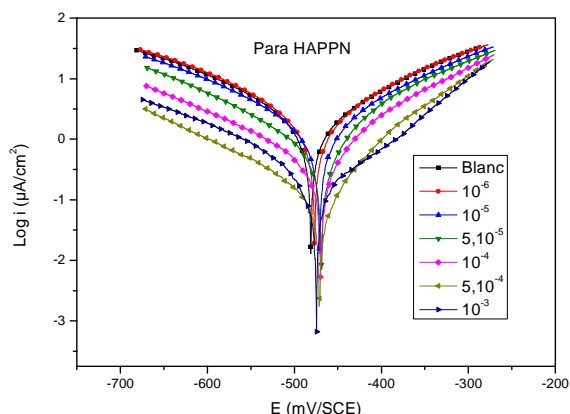


Fig. 8 Polarization curves of steel mild in 1.0 M HCl with and without different concentrations of Para at 308°K

the results reveal that the corrosion current density decrease by increasing the concentration, the lower values in corrosion current was obtained at  $10^{-3}$  concentration with an inhibition efficiency goes until 96% for Para position and 95% for Ortho position. Fig. 7 and 8 shows that Ortho act as cathode type inhibitor while Para act as a mixed type inhibitor.

Table 5: Polarization parameter for the corrosion of steel in HCl 1M acid with and without inhibitors at 308°K

Compounds	Concentration (mol l <sup>-1</sup> )	E <sub>corr</sub> (mV/SCE)	I <sub>corr</sub> (µA/cm <sup>2</sup> )	β <sub>c</sub> (mV/dec)	β <sub>a</sub> (mV/dec)	E <sub>i</sub> %
Blank	0	-482,2	3,3463	-209,9	202,7	-
Ortho	10-6	-479	2,1522	-181	154,4	35,68
	10-5	-481,9	2,1184	-170,4	157,8	36,69
	5.10-5	-485,7	1,9477	-168,4	137,9	41,79
	10-4	-487,8	0,4187	-137,1	108,7	87,48
	5.10-4	-484,8	0,2852	-133,2	93,2	91,47
	10-3	-483,5	0,1577	-166	151,4	95,28
Para	10-6	-476	2,224	-164,3	154,3	33,53
	10-5	-470,8	1,8494	-178,4	153,1	44,73
	5.10-5	-468,9	0,7874	-150,9	98,5	76,46
	10-4	-468,9	0,5149	-172	104,8	84,61
	5.10-4	-471,1	0,2463	-173,6	104,1	92,63
	10-3	-474,7	0,1330	-99,9	104,4	96,02

### 1.7.5. Electrochemical impedance spectroscopy (EIS)

Electrochemical impedance spectroscopy (EIS) becomes a very important tool in the study of the inhibition of corrosion of metals. This method permits to impose a small sinusoidal excitation to an applied potential and then the electrochemical interface metal/solution offers impedance. From the various impedance data, interfaces are often described by equivalent circuits involving resistors, capacitors and sometimes inductances. The various electrochemical reactions involve the formation of electrical double layer. The inhibitive performances of organic inhibitors are widely discussed on the basis of EIS characteristics

The results of the polarization resistance  $R_p$  values of steel in 1 M HCl in the presence and the absence of different concentrations of inhibitors are given in Table 6.

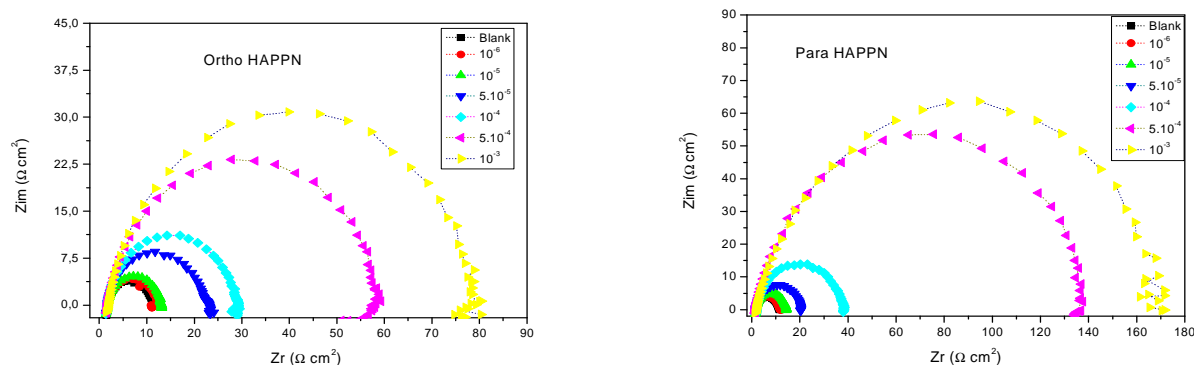


Fig. 9: Impedance diagrams for the corrosion of steel in HCl 1M acid with and without inhibitors at 308°K at Ecorr

Table 6: EIS parameter for the corrosion of steel in HCl 1M acid with and without inhibitors at 308°K

Compounds	C (mol l <sup>-1</sup> )	R <sub>t</sub> (Ω cm <sup>2</sup> )	f <sub>max</sub> (Hz)	C <sub>dl</sub> (μF cm <sup>-2</sup> )	IE <sub>Rt</sub> (%)
Blank	0	9,751	63,29	258,01	—
	10-6	10,57	125,00	120,51	7,74
	10-5	11,35	100,00	140,29	14,08
Ortho	5.10-5	21,31	63,29	118,06	54,24
	10-4	27,28	63,29	92,22	64,25
	5.10-4	54,98	40,00	72,40	82,26
	10-3	75,96	31,64	66,24	87,16
	10-6	9,973	63,29	252,27	2,22
Para	10-5	12,57	79,36	159,62	22,42
	10-5	18,75	63,29	134,18	47,99
	10-4	36,46	40,00	109,18	73,25
	10-4	135,40	20,00	58,80	92,79
	10-3	177,16	20,00	44,94	94,49

The charge-transfer resistance were calculated from the difference in impedances between low and high frequencies [14] and the double layer capacitance ( $C_{dl}$ ) was obtained at the frequency  $f_{max}$  at which the imaginary component of the impedance is maximal ( $-Z_{i,max}$ ) and calculated by the following equation:

$$C_{dl} = \frac{1}{2\pi f_{max} R_t} \quad (14)$$

As observed in Fig.9, the impedance diagrams consist of one large capacitive loop. The high inhibition efficiency enhance  $R_t$  values in acidic medium, and so on the corrosion of steel will be controlled by the charge-transfer process. Values of double layer capacitance decrease in the presence of inhibitors. This result is due to the adsorption of inhibitors on the metal surface leading to the formation of film form acidic solution[15].

## 2. Theoretical results and dissuasions

Quantum chemical calculations have been widely used to study reaction mechanisms. They have also been proved to be a very powerful tool for studying properties of molecules [24-26]. It has been found that the physical properties can be related to its electronic and spatial molecular structure [27-28]. In this study, the relationship between quantum chemical parameters and thermal behaviour of HAPPN Ortho and Para was investigated, using the 6-31G basis; all calculations were carried out by the Gaussian 03. The quantum chemical study is a great method to predict the effectiveness of an inhibitor by its spatial molecular, as well as with their molecular electronic structure, according to Nnabuk O. Eddy and all [19]. Density functional theory (DFT) has provided a very useful framework for developing new criteria for rationalizing, predicting, and eventually understanding many aspects of chemical processes [23]. For this reason quantum chemical study became a common practice to performe theoretical calculations in corrosion inhibition studies. Fig.s 10 shows full geometry optimization of the inhibitors molecules.

The following Table 7 represent the distribution of two enrgies HOMO and LUMO for both inhibitors position isomers, the gap energy ( $\Delta E$ ) and the dipole moment ( $\mu$ ) from the inhibitor to the metal surface

Table7: Parameters Quantum chemical of Ortho and Para HAPPN

Quantum Parameters	Ortho	Para
$E_{\text{HOMO}}$ (eV)	-0.22648	-0.19337
$E_{\text{LUMO}}$ (eV)	-0.01646	-0.00566
$\Delta E_{\text{gap}}$ (eV)	0.21002	0.18771
$\mu$ (debye)	3.4999	2.4010

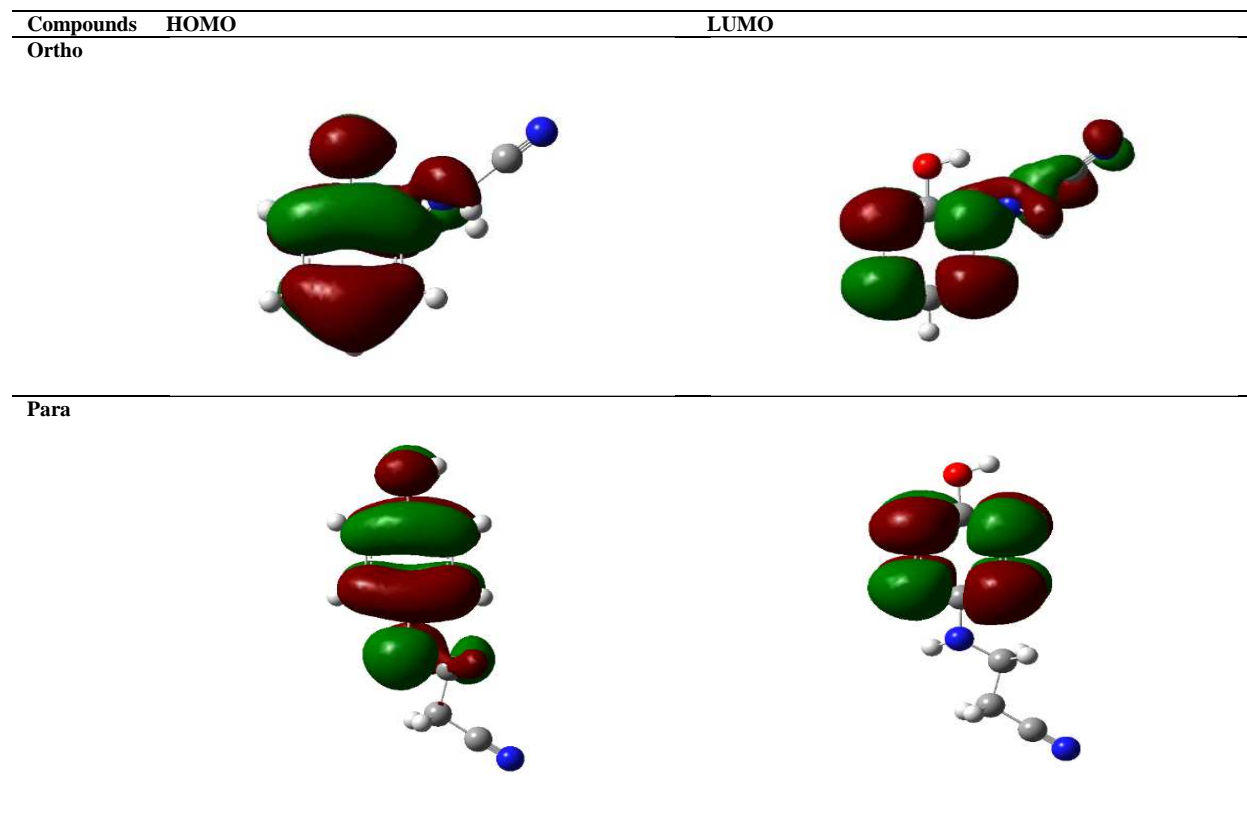


Fig.10 Optimized structure of HAPPN Ortho and Para

The frontier orbital (highest occupied molecular orbital HOMO and lowest unoccupied molecular orbital LUMO) of a chemical species are very important in defining its reactivity. Fukui first recognized this. The energy of HOMO is often associated with the electron donating ability of a molecule. High value of  $E_{\text{HOMO}}$  is likely to indicate a tendency of the molecule to donate electron to appropriate acceptor molecules with low energy empty molecular orbitals. A good correlation has been found between the speeds of corrosion and  $E_{\text{HOMO}}$  that is often associated with the electron donating ability of the molecule. Survey of literature shows that the adsorption of the inhibitor on the metal surface can occur on the basis of donor–acceptor interactions between the  $\pi$ -electrons of the heterocyclic compound and the vacant d-orbital of the metal surface atoms [29-30], Increasing values of  $E_{\text{HOMO}}$  facilitate adsorption and therefore enhance the inhibition efficiency, by influencing the transport process through the adsorbed layer. Therefore, the energy of LUMO indicates the ability of the molecule to accept electrons. The lower is the value of  $E_{\text{LUMO}}$ ; the more probable it is that the molecule accepts electrons. Consequently, less negative HOMO energy and smaller energy gap ( $E_{\text{HOMO}} - E_{\text{LUMO}}$ ) are reflected in a stronger chemisorptions bond and perhaps greater protection efficiency. Concerning the larger values of the energy difference will provide low reactivity to a chemical species. Lower values of the  $\Delta E$  will render good inhibition efficiency, because the energy required to remove an electron from the lowest occupied orbital will be low [31-32].  $E_{\text{HOMO}}$  and  $E_{\text{LUMO}}$  of the inhibitor molecule are related to the ionization potential (I) and the electron affinity (A), respectively. The ionization potential and the electron affinity are defined as  $I = -E_{\text{HOMO}}$  and  $A = -E_{\text{LUMO}}$ , respectively.

It has also been found that an inhibitor does not only donate an electron to the unoccupied d orbital of the metal ion but can also accept electrons from the d orbital of the metal leading to the formation of a feedback bond. Therefore, the tendency for the formation of a feedback bond would depend on the value of  $E_{\text{LUMO}}$ . The lower the  $E_{\text{LUMO}}$ , the easier is the acceptance of electrons from the d orbital of the metal [32]. Based on the values of  $E_{\text{LUMO}}$ , the order

obtained for the decrease in inhibition efficiency (Para >Ortho) was also similar to the one obtained from experimental results.

For dipole moment ( $\mu$ ), lower values of ( $\mu$ ) will favour accumulation of the inhibitor [33-34]. Meanwhile, several authors state that the inhibition efficiency increases with increasing values of the dipole moment [35]. It is worth noting that the experiment showed that the substitute fixed on the HAPPN Ortho and Para does not have much effect on the inhibition efficiency. Ultimately we can conclude for these isomers of position Relationships between inhibition efficiency and the local quantum chemical parameters. The energy levels of frontier orbitals indicate the tendency to form bonds to the metal surface. Further study on chelation centre inhibitors requires information on the spatial distribution of the electron density of these compounds [36, 37]. The structure of molecules can affect the adsorption by influencing the electron density of the functional group.

### CONCLUSION

- The HAPPN position isomers shows that the Para position is efficient than Ortho position in 1 M HCl medium.
- The inhibition efficiency of HAPPN in Para position reaches until 85% at  $10^{-3}$  M.
- The inhibition of corrosion decrease with the rise of temperature.
- Both HAPPN position isomers in Para and Ortho position obey to Langmuir adsorption isotherm.
- The adsorption process is spontaneous and chemically adsorbed (chemisorptions) on the steel surface and is due to adsorption of the inhibitors molecules on the steel surface which is blocking it's active sites.
- The density distributions of the frontier molecular orbital (HOMO and LUMO) show that Ortho and Para adsorb through the actives centres nitrogen and  $\pi$  electrons of the benzene ring.

### REFERENCES

- [1] R. S. Abdel Hameed, H. Abd-Alhakeem, H. Abu-Nawwasb, H. A. Shehata. *Advances in Applied Science Research*, **2013**, 4(3), 126.
- [2] M. Mihit, L. Bazzi, R. Salghi, B. Hammouti, S. El Issami, E. Ait Addi. *International Scientific Journal for Alternative Energy and Ecology*, **2008**, 6 (62), 35
- [3] Li. Xianghong, S. Deng, H. Fu. *Materials Chemistry and Physics*, **2009**, 115, 815.
- [4] A. Zarrouk, B. Hammouti, A. Dafali, H. Zarrok, *Der Pharma Chim.* **2011**, 3, 266.
- [5] L. Herrag, B. Hammouti, S. Elkadiri, A. Aouniti, C. Jama, H. Vezin, F. Bentiss. *Corrosion Science*, **2010**, 52(9), 3042.
- [6] L. Herrag, B. Hammouti, A. Aouniti, S. El Kadiri, R. Touzan, *Acta Chim. Slov.* **2007**, 54, 419.
- [7] L. Malki Alaoui, B. Hammouti, A. Bellaouchou, A. Benbachir, A. Guenbour, S. Kertit, *Der Pharma Chim.* **2011**, 3, 353.
- [8] N. Lahhit, A. Bouyanzer, J.-M. Desjobert, B. Hammouti, R. Salghi, J. Costa, C. Jama, F. Bentiss, L. Majidi. *Portugaliae Electrochimica Acta*, **2011**, 29(2), 127.
- [9] O. Senhaji, R. Taouil, M. K. Skalli, M. Bouachrine, B. Hammouti, M. Hamidi, S.S. Al-Deyab. *Int. J. Electrochem. Sci.*, **2011**, 6, 6290.
- [10] A. Eddib, M. Hamdani, *Mor. J. Chem.*, **2014**, 2 (3), 165.
- [11] H. Zarrok, A. Zarrouk, R. Salghi, M. Assouag, B. Hammouti, H. Oudda, S. Boukhris, S. S. Al Deyab, I. Warad, *Der Pharmacia Lettre*, **2013**, 5 (2), 43.
- [12] M. Bouklah, N. Benchat, B. Hammouti, A. Aouniti, S. Kertit. *Materials Letters*, **2006**, 60, 1901.
- [13] A. Zarrouk, B. Hammouti, H. Zarrok, S.S. Al-Deyab, M. Messali. *Int. J. Electrochem. Sci.*, **2011**, 6, 6261.
- [14] A. Chetouani, B. Hammouti, A. Aouniti, N. Benchat, T. Benhadda. *Progress in Organic Coatings*, **2002**, 45, 373.
- [15] M. Elayyachy, B. Hammouti, A. El Idrissi, A. Aouniti. *Portugaliae Electrochimica Acta*, **2011**, 29(1), 57
- [16] M. Tourabi, K. Nohair, A. Nyassi, B. Hammouti, A. Chetouani, F. Bentiss, *Mor. J. Chem.*, **2013**, 1(2), 33.
- [17] L. Bammou, R. Salghi, A. Zarrouk, H. Zarrok, S. S. Al-Deyab, B. Hammouti, M. Zougagh, M. Errami. *Int. J. Electrochem. Sci.*, **2012**, 7, 8974.
- [18] O. Mokhtari, I. Hamdani, A. Chetouani, A. Lahrach, H. El Halouani, A. Aouniti, M. Berrabah. *J. Mater. Environ. Sci.* **2014**, 5 (1), 310.
- [19] Nnabuk O. Eddy, Eno E. Ebenso. *Int. J. Electrochem. Sci.*, **2010**, 5, 731.
- [20] M. El M. Hamidi, L. Kacha, S. M. Bouzzine, M. El Amane, *Mor. J. Chem.* **2014**, 2(3), 225.
- [21] H. Zarrok, H. Oudda, A. Zarrouk, R. Salghi, B. Hammouti, M. Bouachrine. *Der Pharma Chemica*, **2011**, 3 (6), 576.

- [22] H. Elmsellem, A. Aouniti, M. Khoutoul, A. Chetouani, B. Hammouti, N. Benchat, R. Touzani and M. Elazzouzi. *J. Chem Pharmaceutical Resea*, **2014**, 6(4), 1216.
- [23] P. Udhayakalaa, T. V. Rajendiranb, S. Gunasekaran. *J Adv Scient Res*, **2012**, 3(2): 71-77
- [24] Z. Tao, S. Zhang, W. Li, B. Hou, *Ind. Eng. Chem. Res*, **2010**, 49, 2593.
- [25] K. C. Emregul, M. Hayvali, *Corros. Sci.*, **2006**, 48, 797.
- [26] K. F. Khaled, S. K. O. Babić, N. Hackerman, *Electrochim. Acta*, **2005**, 50, 2515.
- [27] F. Bentiss, M. Lebrini, M. Lagren'ee, M. Traisnel, A. Elfarouk, H. Vezin, *Acta Chem.*, **2007**, 52, 6865.
- [28] C. Hansch, A. Leo, Wiley: New York, NY, USA (**1979**).
- [29] W. Li, X. Zhao, F. Liu, J. Deng, B. Hou, *Mater. Corros.* **2009**, 60, 287.
- [30] R. Hasanov, M. Sadikoglu, S. Bilgic, *Appl. Surf. Sci.* **2007**, 253, 3913.
- [31] M. A. Amin, K. F. Khaled, S. A. Fadl-Allah, *Corros. Sci.*, **2010**, 52, 140.
- [32] H. Wang, X. Wang, H. Wang, L. Wang, A. Liu, *J. Mol. Model.* **2007**, 13, 147.
- [33] T. Mizuno, M. Kitaichi, *Denki Kagaku*, **1993**, 61, 589
- [34] Y. Xu, H. W. Pickering, *J. Electrochem. Society*, **1993**, 140, 658.
- [35] C. Deslouis, M. C. Lafont, N. Pebere, D. You, *Corros Sci*, **1993**, 34, 1567.
- [36] N. Boussalah, R. Touzani, F. Souna, I. Himri, A. Hakkou, S. Ghalem, S. El Kadiri, *J. Saudi Chemical Society*, **2011**, 10, 1016.
- [37] N. Boussalah, R. Touzani, I. Bouabdallah, S. El Kadiri, S. Ghalem, *International journal of Academic Research*, 2(1), 137 (**2009**).